Role of Praseodymium on Zirconia Phases Stabilization

Anna Bonamartini Corradi, Federica Bondioli,* and Anna Maria Ferrari

Department of Materials and Environmental Engineering, University of Modena and Reggio Emilia, Via Vignolese 905/a, 41100 Modena, Italy

Received March 9, 2001. Revised Manuscript Received September 12, 2001

The system zirconia−praseodymia (Pr content 0−15 mol %) has been investigated to evaluate the praseodymium solubility and its role in the zirconia phase stability. The powders have been synthesized by coprecipitation and subsequent calcination at different temperatures (400−1000 °C) for 2 h. The crystal structure of the obtained nanocrystalline (Zr, Pr)-O_2 powders has been studied by X-ray diffraction. By applying the Rietveld method, the dopant effect on the zirconia phase stability was found and discrimination between the different zirconia polymorphs was possible.

Introduction

Over the years, ZrO_2 ceramics have been largely used because of their chemical and physical properties such as excellent chemical resistance, refractory qualities, and ionic conductivity. However, the use of pure zirconia causes remarkable technological problems. It is well known that at atmospheric pressure, pure zirconia presents three polymorphs with monoclinic (20−1170 °C, $P2_1/c$ space group), tetragonal (1170−2370 °C, $P4_2/nmc$ space group), and cubic (2370−2680 °C, $Fm\bar{3}m$) symmetries.[1−3] The characteristics of the monoclinic-tetragonal transformation have important implications regarding the industrial use of zirconia. The volume instability that occurs during transformation results in severe microcracking of pure zirconia. This has been resolved by solid-solution formation, generally obtained with impurities or adding CaO, MgO, or Y_2O_3, which stabilize the tetragonal or cubic structure over a broad-temperature range. Studies on new dopant agents capable of producing powders with improved physical and chemical properties are still of great interest. Doping of aliovalent oxides leads to both an increase in the oxygen vacancy concentration and an enhancement of the oxygen-ion conductivity which enables the usage of this stabilized zirconia as an electrolyte in the fuel cells. Moreover, praseodymium has been chosen being one of the materials under investigation in the field of oxygen-storage materials because it undergoes oxygen exchange at a lower temperature than cerium oxide[4] and its oxygen-storage capacity is not diminished by high temperature of sintering.[5]

The aim of this work has been to verify both the solubility of the praseodymium ion into the zirconia lattice and its influence on the zirconia phase stability. The possibility of PrO_x−ZrO_2 solid-solution formation has been hypothesized, being of unknown phase diagram, on the basis of the lanthania-zirconia phase diagram.[6] The studies regarding this range of composition (Pr content $x = 0$−15 mol %) are few, and the existing ones always involve the use of zirconia already stabilized by other cations, that is, by calcium,[7] yttrium, or cerium.[8] Otherwise, Dariol et al.,[9] by using a pyrolysis process starting from zirconium acetylacetonate and praseodymium oxide (Pr content 5 mol %), have found that praseodymium is not soluble in the zirconia lattice.

In particular, one of the most notable characteristics of some compositionally homogeneous zirconia-based solid solutions is the existence of three tetragonal forms (the so-called t, t', and t"-forms), all belonging to the $P4_2/nmc$ space group.[10] The t-form, stable at high temperature, appears as a tetragonal phase in the equilibrium or stable phase diagram; the t'-form is metastable even at high temperature, and it is unstable in comparison with the mixture of the t-form and the cubic phase. Finally, the t"-form is defined as a tetragonal form without tetragonality (i.e., $c/a = 1$) but with the oxygen atoms displaced along the c axis from their ideal sites of the fluorite-type cubic phase (8c sites of the $Fm\bar{3}m$ space group). This t"-form and the cubic phase are difficult to distinguish. In this work, we have applied the Rietveld method to discriminate between these phases by refining the fractional z coordinate of the oxygen ion in the tetragonal asymmetric unit.[11]

Experimental Section

Sample Preparation. Amorphous zirconia hydroxides containing the amount of praseodymium ion in the 0−15 mol%

* To whom correspondence should be addressed.

(1) Fisher, G. *Am. Ceram. Soc. Bull.* **1986**, *65* (10), 1355.
(2) Howard, C. J.; Hill, R. J.; Reichert, B. E. *Acta Crystallogr., Sect. B* **1988**, *44*, 116.
(3) Smith, D. K.; Cline, C. F. *J. Am. Ceram. Soc.* **1962**, *45*, 249.
(4) Narula, C. K.; Allison, J. E.; Bauer, D. R.; Gandhi, H. S. *Chem. Mater.* **1996**, *8*, 984.
(5) Logan, A. D.; Shelef, M. *J. Mater. Res.* **1994**, *9*, 468.
(6) Lefevre, J. *Ann. Chim. (Paris)* **1963**, *8* (1−2), 117.
(7) Badenes, J.; Llusar, M.; Vincent, J. B.; Cordoncillo, E.; Carda, J.; Monròs, G. In *Key Engineering Materials*; Abelard, P., Autissier, A., Bouquillon, A., Haussonne, J. M., Mocelin, A., Raveau, B., Thevenot, F., Eds.; Trans Tech Publications: Switzerland, 1997; Vols. 132−136, p 53.
(8) Ferrari, A. M.; Corradi, A. B.; Bondioli, F.; Anselmi Tamburini, U.; Gualtieri, A. F. In *Materials Science Forum*; Abelard, P., Autissier, A., Bouquillon, A., Haussonne, J. M., Mocelin, A., Raveau, B., Thevenot, F., Eds.; Trans Tech Publications: Switzerland, 2000;Vols. 321−324, p 932.
(9) Dariol, G.; Poletto, A.; Genel Ricciardiello, F.; Kucich Podda, L. In *Key Engineering Materials*; Abelard, P., Autissier, A., Bouquillon, A., Haussonne, J. M., Mocelin, A., Raveau, B., Thevenot, F., Eds.; Trans Tech Publications: Switzerland, 1997; Vols. 132−136, p 771.
(10) Yashima, M.; Morimoto, K.; Ishizawa, N.; Yoshimura, M. *J. Am. Ceram. Soc.* **1993**, *76* (7), 1745.
(11) Lamas, D. G.; Walsöe de Reca, N. E. *Mater. Lett.* **1999**, *41*, 204.

10.1021/cm010212a CCC: $20.00
Published on Web 11/30/2001

range were prepared by coprecipitation. These hydroxides gels were coprecipitated at pH 9 with ammonia 1 M (NH_4OH, RPE, Carlo Erba, Milan, Italy) from zyrconil chloride (1M, $ZrOCl_2 \cdot 8H_2O$, RPE, Carlo Erba, Milan, Italy) and praseodymium nitrate ($Pr(NO_3)_3$, RPE, Carlo Erba, Milan, Italy) solutions. The amorphous coprecipitated hydroxides, carefully washed with distilled water, were dried in conventional furnaces at 120 °C and then were ground in to an agate mortar. The obtained powders (hereafter indicated for the praseodymium content as Zr0, Zr1, Zr10, and Zr15) were calcined in air, in an electric furnace, for 2 h at different temperatures in the range 400−1000 °C.

Sample Characterization. Thermal behavior of the dried samples was studied by thermogravimetric and differential thermal analysis in air at a heating and cooling rate of 20 °C/min, using a simultaneous TG/DTA apparatus (Netzsch STA409, Selb, Germany). Crystalline phase identification was performed using a computer-assisted conventional Bragg−Brentano diffractometer using CuKα monochromatic radiation (XRD, Philips PW 3710, The Netherlands). The bulk-heated samples were ground to less than 20 μm, and XRD patterns were collected in the 20−70° 2θ range at room temperature. The scanning rate was 0.004°/s, step size 0.02°.

Rietveld analysis of X-ray powder diffraction data has been conducted on the synthesized samples to confirm the solid-solution formation determining the effect of the doping ion on the unit-cell parameters and to quantify the percentage of the crystalline zirconia phases present.[12,1312−13] Powder patterns were collected in the 10−110° 2θ angle range. Refinements were performed using GSAS.[14] In the first cycles, we have refined lattice constants, background parameters, instrumental effects, phase fractions, and profile coefficients of the pseudo-Voigt function modeling of the diffraction peaks. The background function was fitted with a cosine Fourier series function using a six-parameter polynomial in $2\theta^m$, where m is a value from 0 to 5 with 6 refined coefficients. The later stages have been devoted to the refinement of the thermal parameters, fractional z coordinate of the oxygen atom, z(O) for the tetragonal phases. The Zr−O distances were initially constrained, and then the weight of such soft constraints was progressively decreased to zero.

Sample morphology was examined by transmission electron microscopy, TEM (Philips EM400, The Netherlands). Specimens were prepared by dispersing the as-obtained powders in distilled water and then placing a drop of suspension on a copper grid with a transparent polymer, followed by drying. To evaluated the particle-size distribution, maximum diameter of more than 100 particles in the TEM micrographs were measured.

The specific surface area of dried coprecipitated hydroxides was measured by the BET method (Micromeritics, Gemini 2360, Georgia USA), using nitrogen as the adsorbate. The powder density was determined by a picnometry (Micromeritics, Accupit 1330, Georgia USA).

To confirm that solid-solution formation had taken place, leaching tests in boiling solutions of concentrated (36 wt %) hydrochloric acid were performed.[15] The Pr content of the solutions was determined by ICP spectroscopy (Variant, mod. Liberty 200, Australia).

Results

Powder Characterization. TG and DTA analysis of the dried Zr0, Zr1, Zr10, and Zr15 samples (Figure 1) indicates for all the samples a strong endothermic

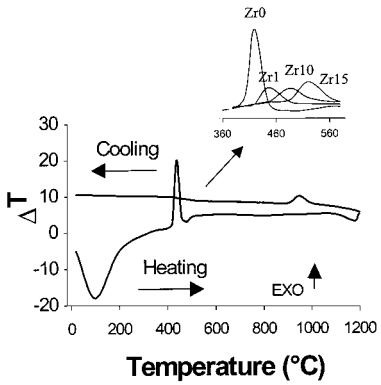

Figure 1. DTA curve of sample Zr0 and crystallization peaks of Zr0, Zr1, Zr10, and Zr15.

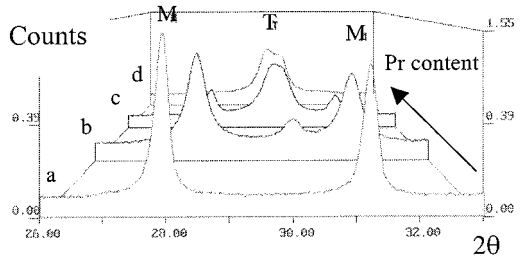

Figure 2. Details of X-ray diffraction patterns of the Zr0 (a), Zr1 (b), Zr10 (c), and Zr15 (d) powders (1000 °C, 2 h).

weight loss corresponding to the dehydration process at a temperature of about 100 °C.

The sharp, exothermic peak at about 450−500 °C is not related to a weight loss and is attributed to the crystallization of pure tetragonal ZrO_2[16] and praseodymia-doped tetragonal zirconia, respectively.[17] In particular, the crystallization temperature of tetragonal zirconia increases with the addition of praseodymium from about 420 to 520 °C. The asymmetry of the exothermic peak increased from the pure Zr0 precursors to the Zr15 sample, which indicates a certain heat release associated, probably, with the enthalpy of the tetragonal solid-solution formation. At higher temperature, only the pure Zr0 sample shows at around 1200 °C the endothermic monoclinic-tetragonal reaction that, for the typical hysteresis effect, on cooling occurs at lower temperature (900 °C).

The stabilizing effect of the praseodymium ion on the zirconia tetragonal phase, by forming the (Zr, Pr)O_2 solid solution, is evidently underlined by X-ray diffraction. Figure 2 clearly shows that the tetragonal phase in the samples treated at 1000 °C for 2 h increases as the dopant quantity is increased. The stabilization of the tetragonal phase is only due to the ion effect. In fact, a possible stabilization caused by the intrinsic grain-size effect[18] is a common effect in all powders (identical calcination conditions). Figures 3 and 4 report the t-ZrO_2 behavior as a function of the calcining temperature. In the sample with a 1 mol % of dopant ion, the content of praseodymium introduced is not sufficient to completely stabilize tetragonal zirconia. ZrO_2 is partially stabilized by praseodymium and is partially monoclinic or tet-

(12) Bish, D. L.; Post, J. E. *Am. Mineral.* **1993**, *78*, 932.
(13) Young, R. A. *The Rietveld Method. IUCr Monographs on Crystallography 5*; Oxford University Press: Oxford, U.K., 1993.
(14) Larson A. C.; von Dreele, R. B. *GSAS: General Structure Analysis System LANSCE*, MS−H805; Los Alamos National Laboratory: Los Alamos, NM, 1998.
(15) Bondioli, F.; Corradi, A. B.; Manfredini, T.; Leonelli, C.; Bertoncello, R. *Chem. Mater.* **2000**, *12* (2), 324.
(16) Caracoche, M. C.; Dova, M. T.; Lòpez Garcìa, A. R. *J. Mater. Res.* **1990**, *5* (9), 1940.
(17) Duràn, P.; Tartaj, J.; Fernàndez, J. F.; Villegas, M.; Moure, C. *Cer. Int.* **1999**, *25*, 125.
(18) Garvie, R. C. *J. Phys. Chem.* **1978**, *82*, 218.

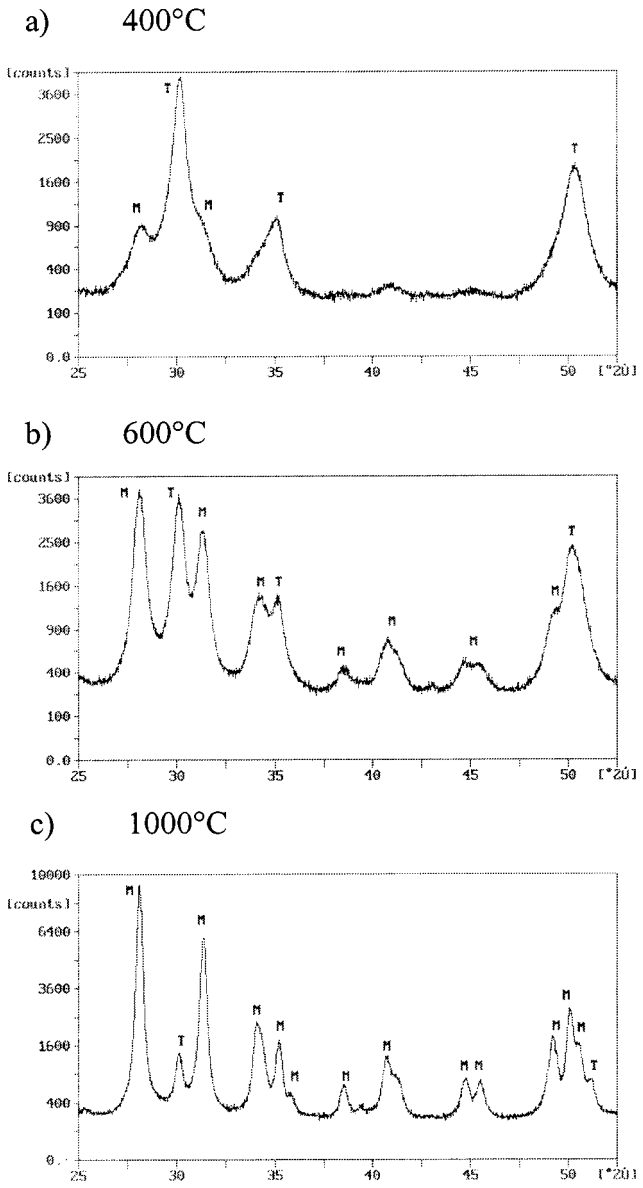

Figure 3. X-ray diffraction pattern of sample Zr1 calcined at 400 (a), 600 (b), and 1000 °C (c) for 2 h.

ragonal, depending on the grain size or on the calcination temperature. In fact, particle size, ϕ, calculated from the specific surface area, S, and density, ρ, using the equation:

$$\phi = \frac{6}{S\rho} \qquad (1)$$

show that at 400 °C and 1000 °C, Zr1 powder has an average particle size of 10 and 56 nm, respectively. These results, confirmed by TEM analysis (Table 1, and Figure 5), are in agreement with the theoretical statement that 30 nm is the maximum grain-size value for the existence of t-ZrO_2 at room temperature. Grain coarsening due to the thermal treatment therefore causes the t→m transition of the zirconia phase which is not stabilized by the doping ion. The behavior of Zr10 powder is closely similar to Zr1, except that a higher amount of praseodymium increases the percentage of stabilized ZrO_2. Further addition of the doping ion in the Zr15 sample results at high temperature in the

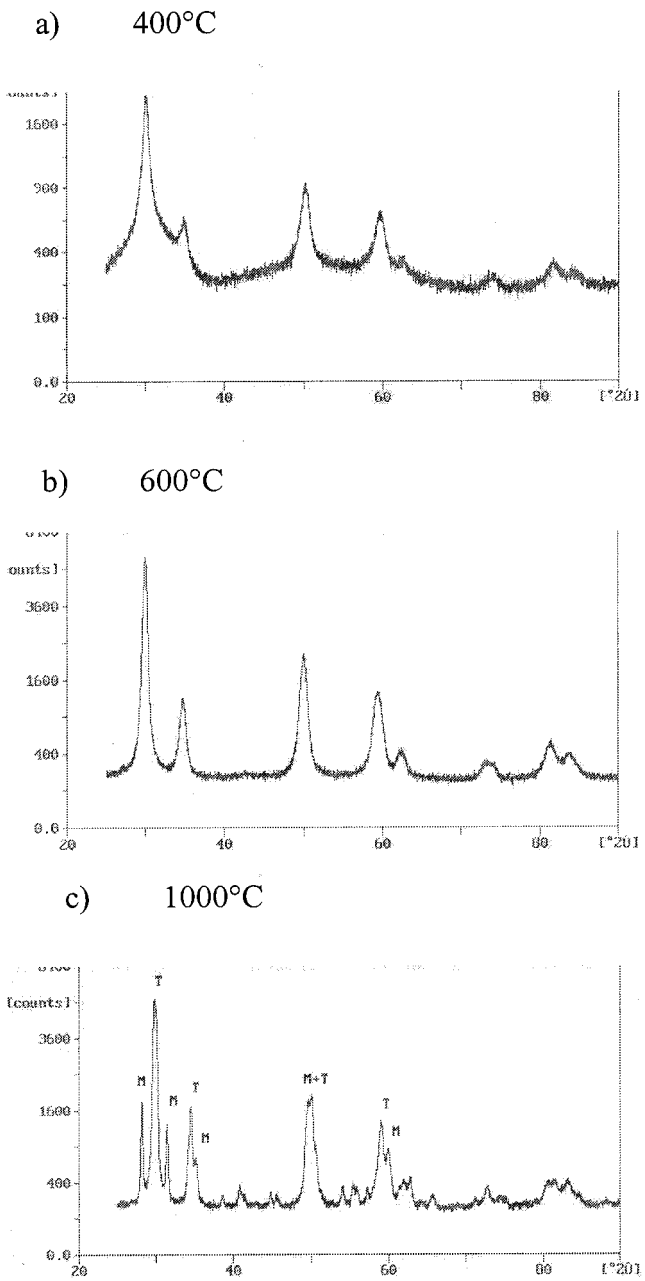

Figure 4. X-ray diffraction pattern of sample Zr10 calcined at different temperatures (2 h).

Table 1. Average Particle Size as a Function of Calcining Temperature and Pr Content (Time 2 h)

sample	temp (°C)	specific surface area (m^2/g)	density (g/cm^3)	average grain size (nm)	TEM average grain size (nm)
Zr0	600	24	5.95	35	28
Zr0	1000	3	5.74	272	n.d.[a]
Zr1	400	100	6.08	9.8	9
Zr1	1000	16	6.50	56	48
Zr10	1000	8	6.63	119	n.d.[a]
Zr15	1000	6	6.84	137	n.d.[a]

[a] n.d. = not determined.

presence of almost exclusively t-ZrO_2. Concerning the powder density (Table 1), the value increases as the praseodymium content is increased.

A confirmation of the solid-solution formation might be obtained by analyzing experimental data of the leaching test performed on the Zr1, Zr10, and Zr15

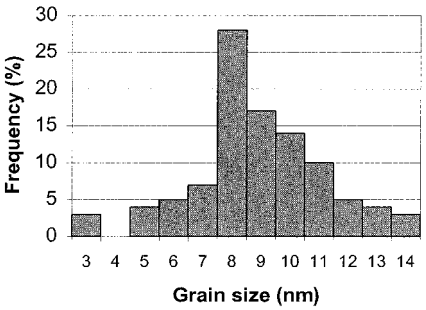

Figure 5. Grain-size distribution as determined by TEM image elaboration (Zr1, 400 °C).

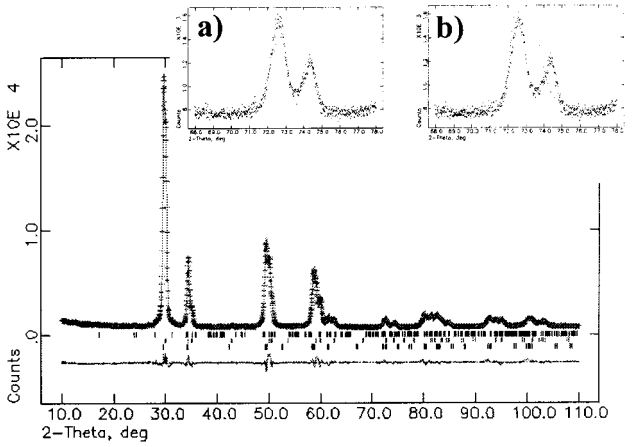

Figure 6. Rietveld fit for the Zr15 pattern with the details of the high-angle region (68−78° 2θ) refinements for (a) the t' + t" model and (b) the t' + c assumption.

Table 2. Pr Release (%) as a Function of Temperature

sample	temp (°C)	Pr (%)
Zr1	400	29
Zr1	600	23
Zr1	800	14
Zr1	1000	4.2
Zr10	400	12
Zr10	600	4.4
Zr10	800	2.8
Zr10	1000	0.5
Zr15	1000	0.8

samples, calcined at different temperatures (Table 2). This selective chemical attack may be considered suitable to evaluate the solid-solution formation, the effective diffusion of praseodymium in the zirconia lattice, and the stability of the powders obtained. The obtained results show that the release of praseodymium decreases as the calcination temperature is increased. In particular, a lower praseodymium solubility is demonstrated in samples calcined at 1000 °C for all the praseodymium contents.

Structural Characterization. The quantitative analysis of the different zirconia polymorphs (cubic (c), tetragonal (t, t', t"), and monoclinic (m)) present in the samples calcined at 1000 °C for 2 h and the effective doping action of the praseodymium ion on the tetragonal zirconia unit cell have been carefully evaluated applying the Rietveld method. In particular, in Zr10 and Zr15 samples, to discriminate between cubic, c, and pseudocubic, t", phases with heavily overlapped reflections, two different starting models t' + c and t' + t" have been used. Figure 6 reports the Rietveld fit for the Zr15 pattern with the details of the high-angle region (68−78° 2θ) refinements for the two-used assumption,[19] thus enabling us to verify the presence of the pseudocubic t" phase. In the t' + t" hypothesis, the refinement proceeded satisfactorily with an agreement index, R_{wp}, of 6.21%, much lower than that of the t' + c model of 13.7%. The obtained results are summarized in Table 3. Atomic coordinates and isotropic thermal parameters of the m-ZrO_2 phase have not been refined since we have verified that they are not useful for the tetragonal/cubic discrimination problem and that they do not affect the

Table 3. Structural Parameters and Standard Rietveld Agreement Factors Obtained for Zr0, Zr1, Zr10, and Zr15 Samples Calcined at 1000 °C for 2 h

	samples			
	Zr0	**Zr1**	**Zr10**	**Zr15**
	m-Phase[a]			
a (Å)	5.1443(1)	5.1501(1)	5.1461(4)	5.1472(2)
b (Å)	5.2084(1)	5.2097(1)	5.2050(4)	5.2047(3)
c (Å)	5.3126(1)	5.3178(1)	5.3142(4)	5.3156(2)
β (°)	99.207(1)	99.145(2)	99.097(5)	99.103
wt %	100(1)	91.51(1)	20.64(9)	1.95(10)
	t′-Phase[b]			
a (Å)		3.6051(2)	3.6135(1)	3.6062(1)
c (Å)		5.1886(3)	5.1955(5)	5.1891(4)
c/*a*		1.018	1.017	1.017
Zr				
x		0.750	0.750	0.750
y		0.250	0.250	0.250
z		0.750	0.750	0.750
U_{iso} (Å^2)		0.0271(5)	0.0216(4)	0.0043(4)
O				
x		0.250	0.250	0.250
y		0.750	0.750	0.750
z		0.208(2)	0.221(1)	0.220(2)
U_{iso} (Å^2)		0.1050(4)	0.0255(7)	0.0087(5)
Zr−O distances (Å)				
Zr−O		2.3547(8)	2.3159(1)	2.3153(9)
Zr−O		2.1009(6)	2.1411(1)	2.1345(8)
wt %		8.49(8)	31.10(10)	29.17(9)
	t″-Phase[b]			
a (Å)			3.6588(2)	3.6735(2)
c (Å)			5.2085(5)	5.2250(5)
c/*a*			1.006	1.006
Zr				
x			0.750	0.750
y			0.250	0.250
z			0.750	0.750
U_{iso} (Å^2)			0.0316(3)	0.0355(3)
O				
x			0.250	0.250
y			0.750	0.750
z			0.246(1)	0.248(1)
U_{iso} (Å^2)			0.1289(4)	0.1194(4)
Zr−O distances (Å)				
Zr−O			2.2561(1)	2.2593(1)
Zr−O			2.2350(1)	2.2485(1)
wt %			48.26(9)	68.88(6)
no. obs. data	4690	5207	4965	5015
no. ref. par.	15	17	16	16
R_{wp} (%)	9.38	6.51	6.40	6.21
R_p (%)	7.17	5.20	5.04	4.77
χ^2	13.00	6.56	5.83	5.56

[a] The structural parameters are from Gualtieri et al.: monoclinic $P2_1/c$ symmetry with fractional atomic coordinates and isotropic thermal parameters: Zr (0.2758(1), 0.04074(8), 0.20798(9), U_{iso} = 0.0087(2) Å^2); O(1) (0.0812(6), 0.3350(5), 0.3442(5), U_{iso} = 0.0075(9)); O(2) (0.4515(6), 0.7537(4), 0.4785(7), U_{iso} = 0.0068(9) Å^2).[21] [b] The structures have tetragonal $P4_2/nmc$ symmetry.

(19) Sanchez-Bajo, F.; Cachadina, I.; de Dios Solier, J.; Guiberteau, F.; Cumbrera, F. L. *J. Am. Ceram. Soc.* **1997**, *80* (1), 232

results. The lattice parameter values clearly show that praseodymium causes an expansion of the primitive cell of t-ZrO_2 phases according to the difference in the ionic radii of Pr^{4+}/Pr^{3+} and Zr^{4+} of 0.90/1.126 and 0.87 Å, respectively.[20] On the contrary, the m-ZrO_2 cell parameters are unaltered with respect to the values reported in the literature for pure zirconia.[21] In particular, it is possible to observe that the limit of praseodymium solubility in the t'-zirconia seems to be around 1 mol %; in the t"-phase, it seems that the limit still has not been reached. In fact, the values of the t"-ZrO_2 lattice parameters increase as the Pr content is increased.

Regarding the quantitative analysis, the monoclinic content considerably diminishes as praseodymium increases favoring the appearance of the tetragonal t' and t" phases. In particular, the tetragonality of the t' and t" phases, which start to appear respectively with a Pr content of 1 and 10 mol %, were estimated to be 1.017−1.018 for the former and 1.006 for the latter, in agreement with Sanchez-Bajo et al. and Sugiyama et al.[19,22] on the yttria partially stabilized zirconia system. Furthermore, considering the noticeable growth of the t" phase, for Zr10 to Zr15 samples, it is possible to suggest that the doping of praseodymium oxide decreases the tetragonality and the t" to t' changeability. The oxygen ion *z* coordinate for t' and t" phases shifts from its ideal value (z(O) = 0.185) for the tetragonal phase in pure ZrO_2 to the limit value of 0.25 for the fluorite type structure.

Discussion

The obtained results show the solubility of praseodymium ion in the tetragonal zirconia structure. The behavior of the tetragonal to cubic phase transition depends on dopant cation (Figure 7). A similar phase change of t' → t" → c with increasing dopant concentration was observed in other systems ZrO_2−$RO_{1.5}$ (R= Y, Nd, Sm, Er, and Yb) and ZrO_2−CeO_2.[23] In this study,

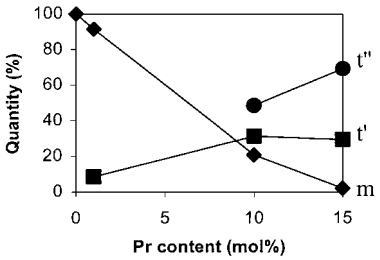

Figure 7. Quantitative behavior of the different zirconia polimorphs (T = 1000 °C, t = 2 h).

we are very distant from the equilibrium conditions being practically impossible to attain phase equilibria at temperature below 1200 °C by the conventional heat treatments because of the slow diffusion of cations.[24] For this reason, we have to refer to the metastable-stable phase diagrams in the ZrO_2−$RO_{1.5}$ systems (R = Y, Sc, and Er).[25] As in these cases, a coexistence region is observed between the tetragonal and monoclinic phases and between the t' and t" forms. In particular, as in the yttria-zirconia system where it is reasonable to interpret that the t"-phorm exists around 14 mol % Y composition,[26] in the praseodymia-zirconia system the t"-ZrO_2 appears between 5 and 10 mol % Pr composition.

Further investigation is necessary to evaluate this metastable phase boundary as well as the effect of praseodymium in ionic conductivity and the correlation between that and structural changes as a function of temperature.

Acknowledgment. The authors thank Dr. Daniele Verucchi who performed the experimental procedure and Dr. Paola Miselli for the assistance in XRD diffraction analysis. In particular, the authors are grateful to Prof. Sanchez-Bajo for interesting suggestions on the Rietveld problems.

CM010212A

(20) Ferrari, A. M.; Corradi, A. B; Bondioli, F.; Anselmi Tamburini, U.; Gualtieri, A. F. In *Materials Science Forum*; Delhez, R., Mittemeijer, E. J., Eds.; Trans Tech Publications: Switzerland, 2000; Vols. 321−324, p 932.

(21) Gualtieri, A.; Norby, P.; Hanson, J.; Hriljac, J. *J. Appl. Crystallogr.* **1996**, *29*, 707.

(22) Sugiyama, M.; Kubo, H. Advances in Ceramics. In *Science and Technology of Zirconia III*; Somiya, S., Yamamoto, N., Yanagida, H., Eds.; American Ceramic Society: Columbus, OH, 1984; Vol. 24, p 965.

(23) Yashima, M.; Takahashi, H.; Ohtake, K.; Hirose, T.; Kakihana, M.; Arashi, H.; Ikuma, Y.; Suzuki, Y.; Yoshimura, M. *J. Phys. Chem. Solids* **1996**, 57, 289.

(24) Stubican, V. S. In *Science and Technology of Zirconia III*; Somiya, S., Yamamoto, N., Yanagida, H., Eds.; Advances in Ceramics 24; American Ceramic Society: Columbus, OH, 1984; p 71.

(25) Yashima, M.; Kakihana, M.; Yoshimura, M. *Solid State Ionics* **1996**, 86−88, 131.

(26) Yashima, M.; Ohtake, K.; Kakihana, M.; Arashi, H.; Yoshimura, M. *J. Phys. Chem. Solids* **1996**, 57, 17.